Quantification of Microemulsion Systems Using Low-Field T1-Weighted Imaging

Herrera Delphine, Thibaud Chevalier, Marc Fleury, Christine Dalmazzone

Quantification of microemulsion systems using low-field T1-weighted imaging.

Delphine Herrera[1], Thibaud Chevalier[1], Marc Fleury[1], Christine Dalmazzone[1].

[1] *IFP Energies nouvelles, 1 et 4 avenue de Bois-Préau, 92852 Rueil-Malmaison Cedex – France*

Corresponding author: Thibaud Chevalier
E-mail address of the corresponding author: thibaud.chevalier@ifpen.fr

Keywords: NMR, quantification, microemulsion, T_1-weighted

Abstract

Applied to Enhanced Oil Recovery, microemulsions are valuable systems for extracting the crude oil trapped by capillary forces in the porous reservoir rocks. The performances of the injected formulations are often assessed by quantifying oil composition in model systems that contain relatively high amount of surfactant/co-surfactant. Recently, the question of representativity of such systems was raised because kinetics aspects and complexity of crude were neglected in model systems and are likely to impact the process efficiency. The current quantification techniques limit the characterization of representative model systems as they are destructive, time consuming and not often applicable to dark or opaque systems. In the original aim to provide a quantitative kinetic study of such microemulsions, we propose a high resolution T_1-weighted imaging technique to have access to 1D-composition profiles of co-surfactant, oil and brine in Winsor I, Winsor III and Winsor II microemulsions. The analysis is carried out on model systems at equilibrium for proof of concept. Results are correlated with X-Ray Micro-Computed Tomography experiments to provide better interpretations and assess the method accuracy. We provide conditions of validity of the developed NMR method and discuss its potential limitations. To a larger extent, the method could be of interest to other applications that use similar systems.

Graphical abstract

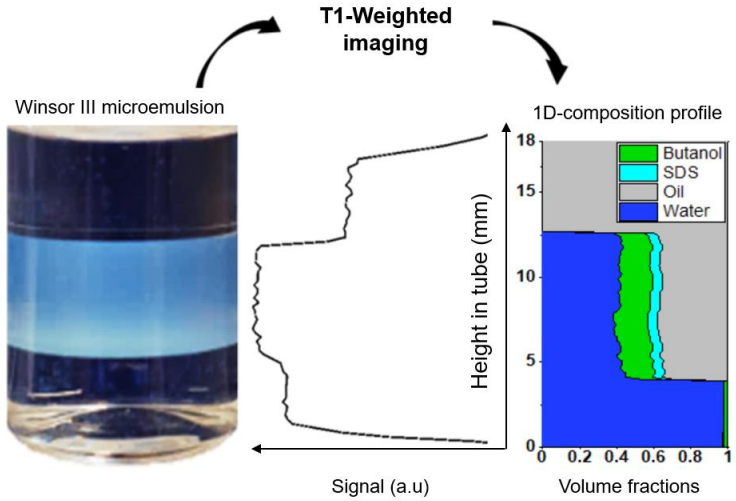

Abbreviations

A	a.u	Absorbance
B	vol.%	Brine composition profile along the tube height
CPMG	NA	Carr-Purcell-Meiboom-Gill sequence
φ_i	None	Volume fraction of species *i*
I_0	a.u	Incident intensity from Micro-CT
I	a.u	Transmitted intensity from Micro-CT
μ_i	m^{-1}	Attenuation coefficient of species *i*
N	vol.%	N-butanol composition profile along the tube height
NMR	NA	Nuclear Magnetic Resonance
ρ_{ap}	a.u	Apparent Hydrogen density at a given height in the sample
ρ	a.u	Total Hydrogen density at a given height in the sample
ρ_i	a.u	Total Hydrogen density at a given height for species i measured separately
P_{ap}		Apparent Hydrogen density distribution along the tube
P	a.u	Total Hydrogen density distribution along the tube
P_i	a.u	Total Hydrogen density distribution along the tube for species i measured separately
RD	s	Relaxation Delay : time allocated to the NMR relaxation process
S	vol.%	Sodium Dodecylsulfate composition profile along the tube height
SDS	NA	Sodium Dodecylsulfate
t	s	Time
T	vol.%	Toluene composition profile along the tube height
T_{1i}	s	T1-Relaxation time in NMR of species *i*
T_{2i}	s	T2-Relaxation time in NMR of species *i*
x	m	Distance in tube
1D	NA	One dimension
WI, WIII, WII	NA	Winsor I, Winsor II, Winsor III

1 Introduction

The characterization of complex fluids is a constant challenge to the oil industry. For many years, research has focused on the characterization of water-in-oil emulsions produced after crude extraction. NMR technique has been widely used not only due to its applicability to dark and viscous systems but also to the wealth of information collected from both a structural and compositional points of view. In the last decades, improvements of the self-diffusion and transverse relaxation techniques enabled to have access to the droplets size distributions [1,2] and the dynamic monitoring of emulsion destabilization [2,3]. In a recent study [4], NMR droplet size distribution measurements and vertical profiles were combined to fully characterize a des-emulsification process involving low viscosity crudes for which T1-relaxation times of crude and water often overlapped. More original works can be encountered in literature such as studies on the rheological properties of emulsions [5], the quantification of aromatics contents in petroleum distillates [6] or even the behavior of asphaltenes at O/W interfaces [7] which further broadens the field of applications of NMR technique.

Nowadays, due to the implementation of Enhanced Oil Recovery processes (EOR), the oil industry faces other complex systems called “microemulsions”. The term “microemulsion” is misleading because they are not emulsions of micro-size droplets but isotropic and thermodynamically stable systems showing low viscosity and interfacial tensions in the range of 10^{-2}-10^{-3} mN/m between oil and water phases [8][9,10]. They are used in a large variety of applications in all chemistry domains such as cosmetic, chemical, drugs, food and oil industries mainly for their high oil solubilization performances and particular structures encountered [11]. For the oil industry, the existence of ultra-low interfacial tensions appears to be a good alternative to extract the spare crude trapped by capillary forces in the porous reservoir. Contrary to classical emulsions, the microemulsions are spontaneously formed after contact of an injected aqueous phase, containing a relatively high amount of surfactants, and an oily phase (i.e. crude). Depending on the nature of the phases in contact and oil/water ratio in the system, three main types of microemulsions can be encountered according to Winsor classification [12]. The Winsor I and II types are in the form of dispersed droplets comparing to the Winsor III type which is bicontinuous and made of highly interconnected water and oil domains that have characteristic sizes of around 10 to 100 nanometers. As anionic surfactants are mostly used in the EOR processes, a co-surfactant (alcohol molecules) is often added to the formulation. The co-surfactant prevents the precipitation of the surfactant at high salinities. As anionic surfactants are mostly used in the EOR processes, a co-surfactant (alcohol molecules) is often added to the formulation. The co-surfactant helps to prevent the precipitation of the surfactant at high salinities. It also enables the formation of the microemulsion by penetrating into the surfactant layer and enhancing the interfacial fluidity. On model systems, a relatively high amount of surfactants and co-surfactant is used compared to real systems. In practice and before upscaling, preliminary works are first carried out on model systems [13–20] to assess the performances of the formulations in static and after flowing conditions namely in terms of oil recovery and effective formation of the microemulsion. Among existing methods to quantify these systems, techniques such as Karl-Fischer and Hyamine titrations or UV-spectroscopy are commonly used as routine tests to assess respectively compositions of water and surfactant in the different phases of the model microemulsion at equilibrium [19,21]. Gas chromatography was successful in characterizing excess oil/water phases as well as

co-surfactant partitions in bicontinuous microemulsions [22–24]. Recently, a new application of Differential Scanning Calorimetry appears to be an alternative to chemical methods for measuring the amount of water in microemulsions giving extra information on water domains sizes due to a correlation between melting temperatures and confinement [25–27]. Nevertheless, all these methods are destructive and the information collected are often limited to one compound or mean compositions.

When applied to microemulsion systems, NMR has been usually used to provide structural information by measuring the self-diffusion coefficients [28,29]. The order of magnitude of the diffusion coefficients in the sample compared to the bulk case enables to distinguish the shape and size of the dispersed objects from spherical micelles to lamellar phases. It is one of the only techniques that was able to directly prove the bicontinuity of Winsor III microemulsions [30]. Relaxation studies have been much less performed on microemulsion because it is poorly sensitive to inter-objects interactions and thus does not give as precise structural information as diffusion coefficients monitoring. In our study, this could be beneficial for quantification purposes given that relaxation times should not be drastically affected from a bulk conformation to a bicontinuous medium for instance.

In our specific application, our aim was to extract compositions and follow the kinetics of formation of microemulsions for process optimization purposes and so, despite their darkness or opacity. However, the techniques described above need sampling and the structure of the system makes it difficult to probe local compositions during microemulsion formation or even at equilibrium. To reach this objective, one needs an analytical technique which allows:

- Simultaneous quantification of a multi-component system
- Fast-responses acquisitions
- Application to all liquid systems independently from their microscopic structures
- Non-destructive measurements
- Application to dark/opaque systems

In that objective, we provide an application of T1-relaxometry that gives simultaneous access to 1D-compositions profiles of each species in microemulsions. Its use could be of interest to those who need a non-destructive, relatively fast quantitative method, well suited to dark / opaque systems and which allows the simultaneous quantification of a multicomponent system. It should be noted that different types of model systems are now used in a large range of applications going from innovative extraction and reaction processes [31–34] to drug delivery systems [24,35–37] and even formulation of cleaner fuels [38–40].

The studied microemulsion is a well-known quaternary system containing Toluene/NaCl Brine/n-Butanol/Sodium Dodecylsulfate [41]. To assess the method, we compared NMR results to X-ray Micro-Computed Tomography (Micro-CT) experiments. In this study, the methodology is described on static compositions of microemulsions chosen at equilibrium for proof of concept. It will be carried out further in dynamic conditions to better understand the mechanisms of microemulsification. We discuss advantages and limitations of the same NMR application. The work particularly focuses on the description of the methodology and could potentially be extended from bicontinuous microemulsions characterization to a wide variety of colloidal systems.

2 Materials and Methods

2.1 Products and microemulsions systems

Sodium Dodecylsulfate surfactant “SDS” (Dry weight 98.5 % - water <1.5 %) was supplied by Alfa Aesar and used without further purification. Toluene is from VWR (AnalaR Normapur), n-butanol and sodium chloride NaCl are from Merck (grade analysis). Milli-Q water was used.

The studied systems are made of NaCl Brine, Sodium Dodecylsulfate “SDS” (surfactant), n-butanol (co-surfactant) as aqueous phase and toluene as oil phase. The aqueous phase is first formulated in the tubes by dissolving SDS in the mixture water and n-butanol. The mixtures are completed with an appropriate volume of concentrated mother solution of brine to attain the desired salinity in the aqueous phase. Toluene is then added gently to the aqueous phase and the tube is turned 3 times up and down to allow phases contact. The tubes are sealed with Teflon rubber and allowed to rest 1 day until equilibrium is reached meaning the thickness of the middle phase is constant over time. Compositions are calculated to satisfy a water to oil volume ratio WOR=1 ; Co-surfactant= 5.5 vol.% of total system; Co-surfactant/SDS weight ratio = 2. A salinity scan as well as interfacial tensions measurements were performed to define the range of Winsor I, Winsor III and Winsor II systems (See in Supporting Information). We probed five salinities to discuss the applicability of the developed NMR method : 30 g/L (Winsor I) ; 48 g/L (Winsor III limit to Winsor I) ; 54 g/L (Winsor III at optimal salinity) ; 63 g/L (Winsor III limit to Winsor II) and 70 g/L (Winsor II). The microemulsions were formulated in glass tubes with a total volume of 3 mL for NMR and 10 mL for Micro-CT. NMR transverse T_2 relaxation times of the above components are listed in Table *1*.

2.2 NMR apparatus and sequences

A bench top of 20 Hz from Oxford Instruments equipped with a 1.8 cm diameter probe was used for the NMR acquisitions. The 3 mL sample was placed in a 1.8 cm-outer diameter glass tube resulting in about 2 cm in height. The temperature is controlled during the experiment and set at 30 °C. The equilibration time of the tube in the environment is 50 min.

The following application requires the T_1 relaxation times of each species of the system (Eq. 3). For this, T_2 relaxation times of separate references (Table *1*) were measured with a CPMG sequence (Carr-Purcell-Meiboom-Gill) with an inter-echo time of 100 to 300 µs. It is commonly accepted that the longitudinal relaxation times $T_1 = T_2$ for such liquid systems. For each species, we thus fixed the value of T_1 to the measured T_2 of the corresponding reference. It leads to consider that relaxation times in-situ the microemulsions are not drastically affected by the internal structures, as already mentioned in the Introduction.

The profile acquisition sequence is described in Figure 1. To have good compromises between signal resolution and fast responses, we average the signal over 4 scans and

2 unrecorded dummy scans leading to a total maximum measuring time of 1.40 min. The relaxation parameter RD corresponds to the time between each scan. The acquisition parameters of the sequence are such that the vertical resolution is 118 µm with a field of view of 3 cm (Figure 1).

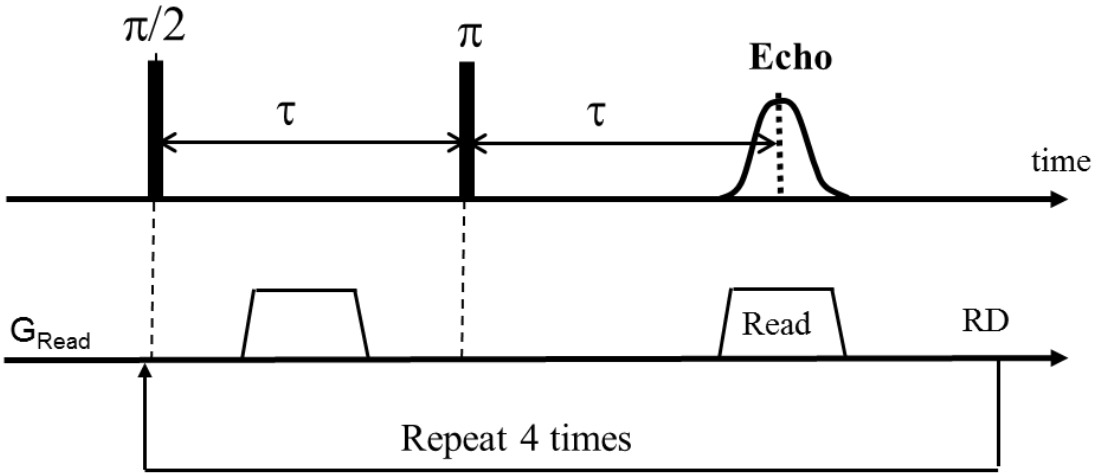

Figure 1: T_1 weighted 1D imaging sequence. The gradient GREAD is along the vertical direction. Acquisition parameters: τ=2 ms, gradient amplitude=8.39 G/cm, filter bandwidth 50 kHz, number of acquired points 128.

2.3 X-ray measurement

The X-Ray Micro-CT tests are conducted on an EasyTom 150-160 from RX Solutions in a 10mL glass tube of 1.8 cm-outer diameter at ambient temperature (~20°C). An X-ray source irradiates the whole tube. The detector is set behind the tube and collects the transmitted X-rays radiations. A 2D-radiography is acquired in function of the height and thickness of the tube as depicted in Figure 6. The time for one acquisition is 5 seconds.

3 NMR method

The objective is to visualize and quantify the three phases present in the systems as a function of height (Figure 2). Especially in the microemulsion located in between the brine and toluene, the quantification of the phases is of prime interest to study the formation and evolution of microemulsions. From density profiles alone, it is not possible to obtain the desired quantities since the hydrogen index of the surfactant (SDS solution), the co-surfactant (n-butanol) and brine are very close (Table *1*). There exists however a large contrast with toluene but it might not be the case in industrial situations in which microemulsions are formed with crude oils. We explain below how we can take advantage of the relaxation time contrast to quantify all phases at any height in the sample.

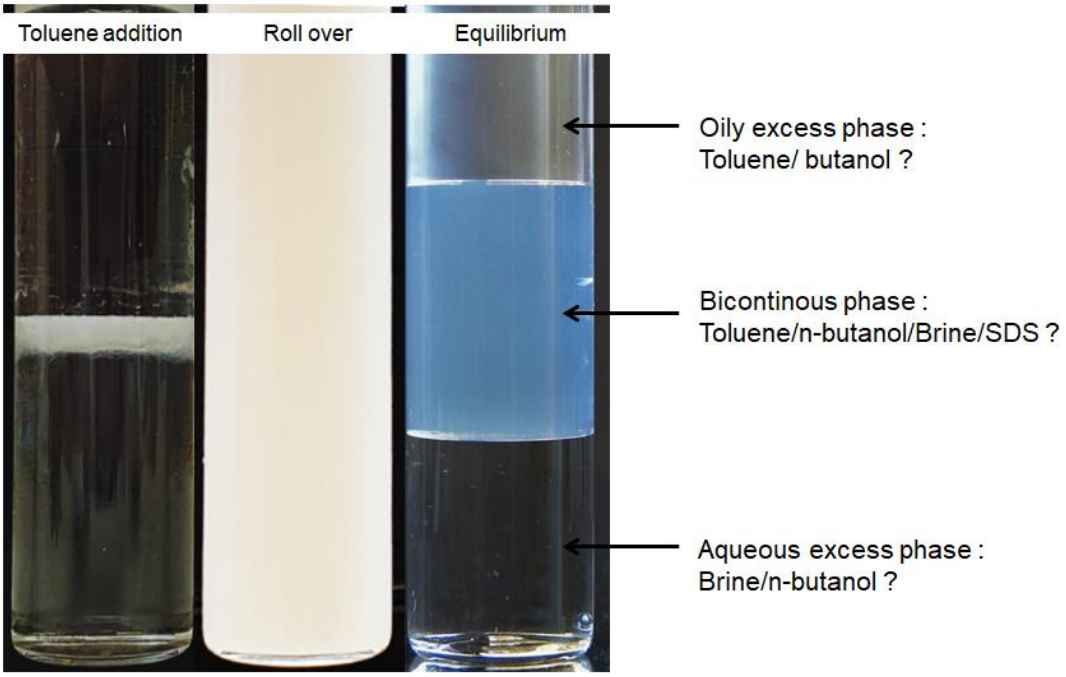

Figure 2: Photographs of the SDS / n-butanol / NaCl brine / Toluene system during each formulation steps: left- after Toluene addition onto the aqueous phase; center- after rollover of the tube; right- at equilibrium at optimal salinity of 54 g/L. The time needed to reach equilibrium was 1 day after rollover and standing at room temperature.

For this purpose, the relaxation delay (parameter RD) in the imaging sequence is tuned adequately to weight the total H-density profile by the longitudinal T_1 relaxation time of each species, as described below and illustrated in Figure 4. To allow quantification, we collect and analyze 2 profiles: fully polarized ($RD \geq 5xT_1$ for all species) and partially polarized ($RD < 5xT_1$ for some species).

At first step, we assess the homogeneity of the magnetic field by measuring the Pure Toluene response over the height required for the study (i.e. 2 cm). The signal response is shown in Figure 3: a flat profile is obtained with an accuracy evaluated at 4% as detailed in Supporting Information. We noticed that interfaces with Air/Toluene and Toluene/Bottom of the tube are not sharply defined. For repeatability conveniences, we choose to extract volume fractions by excluding interfaces effects that is to say in a zone where density profiles are flat (as delimitated by the red lines in Figure 3). This would actually underestimate the volumes of the upper and lower phases. Consequently, after calculations, they should be corrected by the addition of respectively 0.13 mL to the upper oily phase and 0.14 mL to the lower aqueous phase.

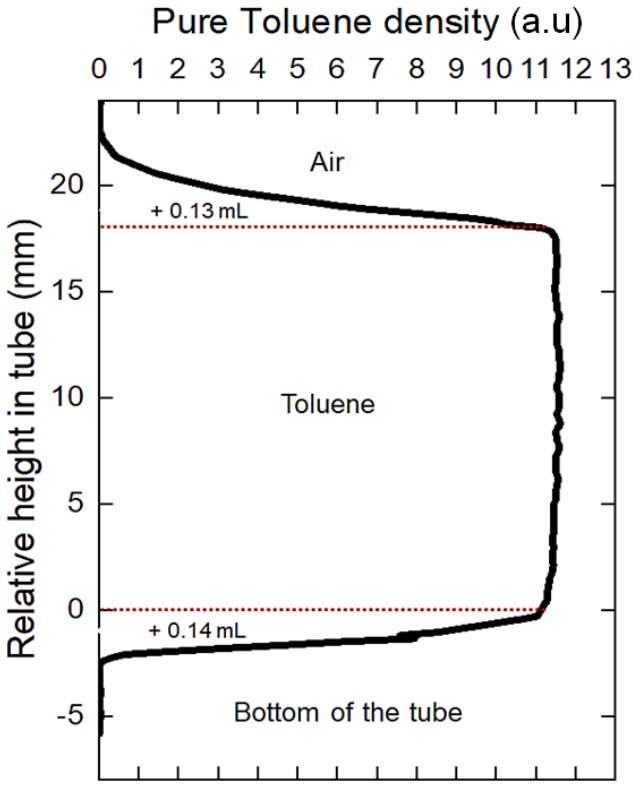

Figure 3: Signal response of pure Toluene and impact of interfaces limits on volume calculations.

3.1 **Parametrization of the sequence**

We introduce ρ and ρ_{ap} as respectively the total and apparent H-density at a given height in the sample. When RD > 5 T_{1i}, set up here at RD=15 s, all protons of the sample have returned to their initial position. Consequently, the collected signal at a given height in the system is called total density ρ and is only dependent on the hydrogen index of the measured local composition (Table 1). In the case of binary systems, a contrast in hydrogen index between the two components would be satisfactory to quantify the volume fractions φ_i for each component based on mixing rules (Eq. 1 and Eq. 2). The total densities ρ_i of each species *i* are obtained by measuring the pure species responses separately. However, for multi-components systems, the two equations are not sufficient for the quantification of volume fractions. Moreover, in practice, when studying organic compounds, the intrinsic hydrogen densities are often too close to distinguish them, which means that the pure references and mixtures samples could have equal total densities. Consequently, the equations lead to non-unique solutions.

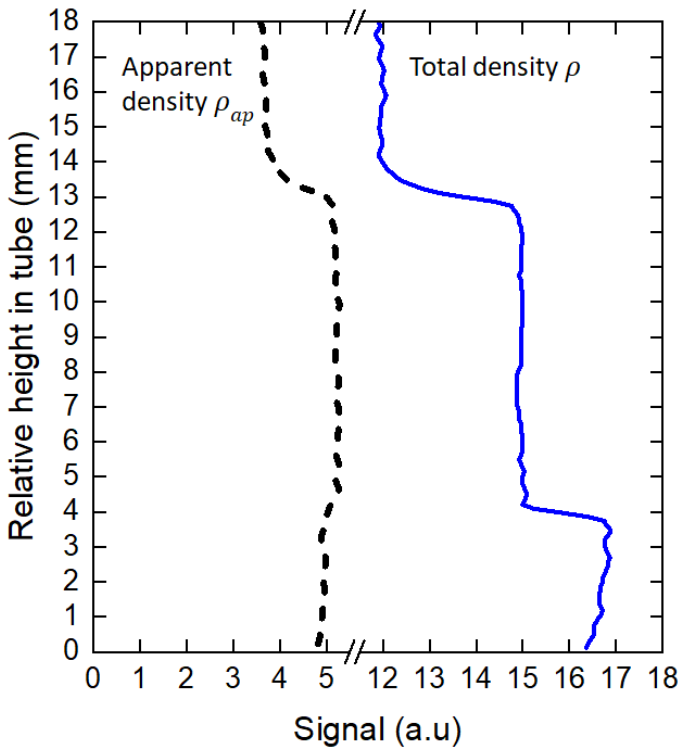

Figure 4: Example of raw profiles for total ρ and apparent ρ_{ap} densities on the equilibrated microemulsion at optimal salinity in function of the relative height in the tube

For this reason, the T1-weighted sequence used is notably sensitive to contrasts in relaxation times T_{1i}. Indeed, for a RD close to T_{1i}, set up here at RD =1 s, the relaxation process is sub-polarized for components i that have T_{1i} > RD. It corresponds to the apparent density ρ_{ap} in Figure 4. The value of RD is chosen at 1 s to have enough contrast between total ρ and apparent density ρ_{ap}. It also permits to have better compromises between the duration of the acquisition and the resolution of the sub-polarized signals. Consequently, the measured apparent density ρ_{ap} collected at a RD =1 s corresponds to a unique composition and follows sharp and detectable variations when local compositions change in the system according to Eq. 3. This new equation and the only knowledge of relaxation times T_{1i} of each species thus permit the quantification of the other compounds in our case. It is worth mentioning that acquisitions in partial relaxation mode at different RD ~ T_{1i} should provide as many additional equations as components in the system according to Eq. 3.

$$\rho(h) = \sum_i \varphi_i \, \rho_i(h) \qquad \textit{Eq. 1}$$

$$1 = \sum_i \varphi_i \qquad \textit{Eq. 2}$$

$$\rho_{ap}(h) = \rho(h)\left(1 - \sum_i \varphi_i \;\; exp^{-RD/T_{1i}}\right) \qquad \textit{Eq. 3}$$

Where ρ_{ap} (or ρ) is the apparent (or total) density in the system at height *h* in the tube for a given RD; φ_i accounts for volume fraction of components *i* in the system at height *h* and ρ_i are the densities of pure species *i* measured separately.

3.2 Application to the model system accounting for the sample's height

In our model case, the system is made of four components: n-butanol, Toluene, brine and SDS. Visually, it is triphasic and can be split from top to bottom into three zones: excess oil phase, bicontinuous microemulsion and excess water phase. At first, we assumed all four components can be encountered in any zone of the tube. By extension along the tube and application to the quaternary system, the equations Eq. 1, Eq. 2 and Eq. 3 are turned into a system of equations (Eq. 4, Eq. 5 and Eq. 6) where the 1x1 matrix T, N, B, S represents respectively, Toluene, N-butanol, Brine, SDS volume fractions distributions along the tube. Details on the system's resolution are explained bellow and illustrated in Figure 5. The signal vertical resolution is 0.1 mm. The data are automatically processed on the Python software from raw profiles.

$$P = T \times P_T + B \times P_B + S \times P_S + N \times P_N \qquad \textit{Eq. 4}$$

$$P_{ap} = P \times (1 - T \times exp^{-RD/T_{1T}} - B \times exp^{-RD/T_{1B}} - S \times exp^{-RD/T_{1S}} - N \times exp^{-RD/T_{1N}}) \qquad \textit{Eq. 5}$$

$$1 = T + B + S + N \qquad \textit{Eq. 6}$$

Where P_{ap} is the 1x1 matrix containing all the values of apparent densities $\rho_{ap}(h)$ along the tube height (with an interval of 0.1 mm). Same considerations for P.

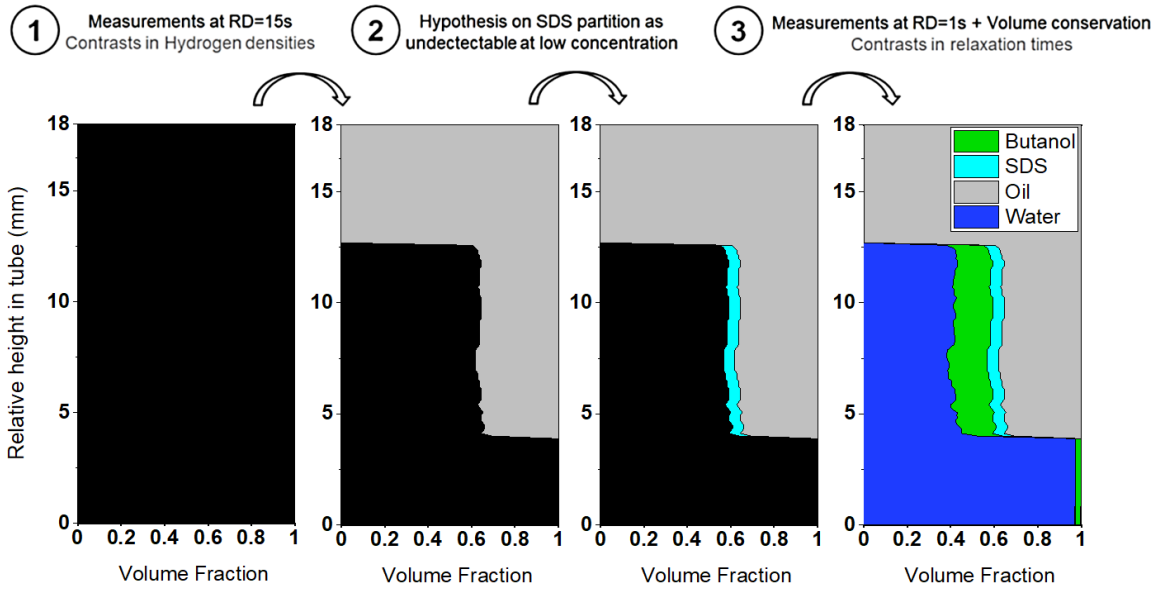

Figure 5 : Schematic description of the system's resolution strategy

3.3 Resolution of the system

We first used the density contrast between toluene and the other species to reduce the number of unknowns. Interestingly, a clear contrast in total density appears between Toluene and the compounds of the aqueous phase. Given the hydrogen index of Table 1, we confirmed that this effect is due to the lower density of protons per cm^3 in Toluene. The contrast enables to directly deduce the distribution of Toluene volume fractions along the tube from the total densities as $P_S \sim P_B \sim P_N$ reducing Eq. 4 to Eq. 7.

$$T = \frac{P - P_B}{P_T - P_B} \qquad \textit{Eq. 7}$$

Second, we assume that the surfactant is mainly located in the microemulsion. The surfactant volume fraction in the system is 2.2 vol.%. The calculated contribution of SDS to the signal in each phase can be deduced from Eq. 5 and does not exceed 3.5 % of the apparent signal. We estimated the method accuracy on the signals, with our input parameters, at +/- 4% and +/- 0.6 % respectively for apparent densities and total densities by carrying out reproducibility and repeatability measurements as detailed in Supporting Information. After data treatment, the precisions on the signals both at RD 1s and RD 15s imply a precision on volume fractions of 4 vol.% at height *h* in the sample. This means SDS at 2.2vol.% could not be quantified properly. Moreover, previous studies are in agreement to say that surfactant molecules concentrate in the microemulsion phase [16,19]. Consequently, we consider that the excess phases do not contain significant amount of SDS. We thus made the hypothesis that SDS is homogeneously distributed in the microemulsion phase for enabling calculations.

Finally, regarding the considerations above, the system is reduced to two unknown variables. By using Eq. 5 and the conservation of volume fractions Eq. 6, we were able to extract n-butanol and brine distribution along the tube thanks to respectively strong contrasts in T_1-relaxation times and the conservation of volume fractions.

3.4 Comparison with X-ray Micro-Computed Tomography (Micro-CT)

The principle is based on the transmission of X-rays radiation through the sample. The absorbance at a given height in the sample varies according to Beer-Lambert law depending on the attenuation coefficient μ_i, volume fraction φ_i of each species *i* (Eq. 8 and Eq. 9) and thickness x. The attenuation coefficients are dependent on the electron densities of the material but also on the energy of the X-ray radiations source. The acquired pictures of transmitted intensities are processed on Image J software to obtain the gray level profile of the sample as depicted in Figure 6. Because of a contrast in attenuation coefficients between water and the two other compounds (Toluene, n-butanol), the technique allows to extract the brine distribution (Eq. 10) along the tube with a spatial pixel resolution of 72.19 µm to be compared to NMR for better method assessment. Micro-CT is not sensitive enough to extract the SDS distribution meaning there is no contrast between a solution of 5 wt.% of SDS in water and water only. Thus, in our specific case, SDS is measured out in the brine quantification. The estimated error on the deduced volume fractions is +/-2 % and mainly because of a beam hardening effect occurring due to the thickness of glass tube.

$$\frac{1}{I} dI = -\sum_i \varphi_i \mu_i \; dx \qquad \textit{Eq. 8}$$

$$A = \ln\left(\frac{I}{I_0}\right) \qquad \textit{Eq. 9}$$

$$\varphi_{brine}(h) = \frac{Ln\,(I_{oil}) - Ln\left(I_{sample}\,(h)\right)}{Ln\,(I_{oil}) - Ln\,(I_{brine})} \qquad \textit{Eq. 10}$$

Where A: absorbance ; I_0: incident intensity ; I: measured intensity ; $\varphi_{brine}(h)$: the volume fraction of brine at height h in the sample, I_{oil} and I_{brine}: the transmitted intensities of separate Brine and Oil reference (n-butanol and/or Toluene).

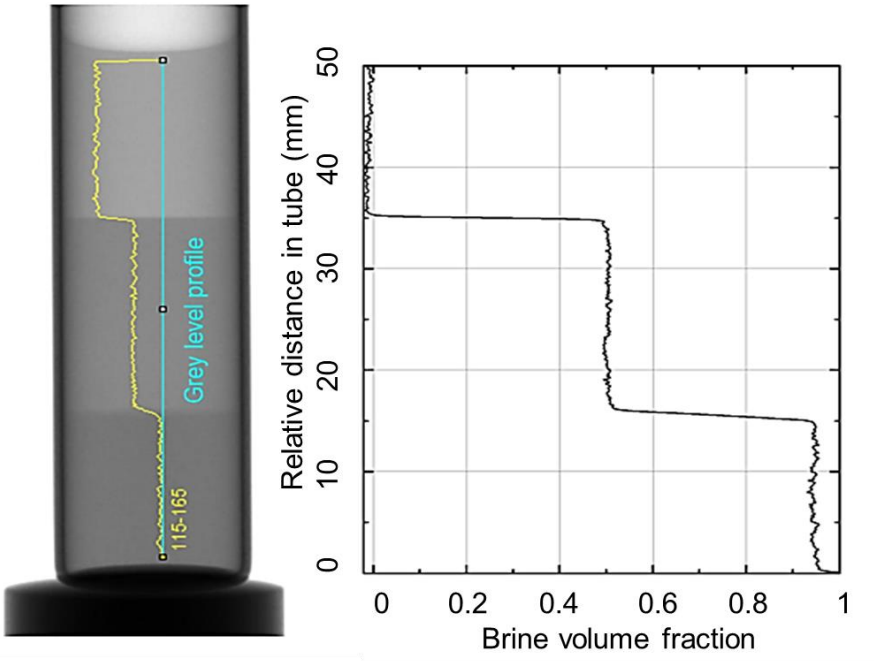

Figure 6 : Example of a Micro-CT radiography of the equilibrated microemulsion at optimal salinity of 54 g/L - Transformation of grey level profile in brine volume fractions along the tube

4 Results

The compositions profiles deduced from NMR are displayed in Figure 7 for each salinity. The irregularities that could be observed on NMR plots are potentially due to the set-up parameters of the sequence. They could be corrected by increasing the number of scans and dummy scans in the sequence, i.e. increasing the time of the acquisition to enhance the precision of the signal. Table 2 shows the mean volume fractions in the microemulsion phase at equilibrium as well as the volume fraction occupied by the phase extracted by NMR and Micro-CT. Signal processing could be performed for all samples of microemulsions, from Winsor I to Winsor III and Winsor II types. Good agreements are found compared to Micro-CT on similar formulations in terms of volume fractions in the middle phase and phases thicknesses as depicted in Table 2, Figure 7 and Figure 8. The results indicate that the deviations between NMR and Micro-CT tends to increase (1 vol.% to 7 vol.%) when the system is far from optimal salinity. Indeed, the change from a bicontinuous to a dispersed structure is likely to slightly affect the relaxation times due to the species confinement. The method is thus more precise on Winsor III systems even still applicable on Winsor I and Winsor II microemulsions. Indeed, some current techniques such as DSC or Karl-Fischer titration can lead to the similar deviations when quantifying microemulsions systems [19,25]. During data processing, we noticed that the NMR brine quantification in the microemulsion phase could be done by two ways. The first one was to consider brine and SDS separately with their respective relaxation times T_1 detailed in *Table 1*, (i.e. as described in the above methodology). The calculation is thus carried out as if the system was made of four-components and we extracted separately the brine and SDS

volume fraction. The second way to quantify brine was to consider a solution made of ~ 5 vol.% of SDS and the relaxation times corresponding to such a solution. By this way, the system in the microemulsion phase is considered as triphasic and we extracted the SDS+Brine volume fraction. Because SDS is estimated by hypothesis, it is thus possible to extract the brine volume fraction only. The two ways of calculations lead to the same composition of brine. In particular, it provides a physical meaning of the implemented volume fraction of SDS: it is a water-soluble surfactant and thus it can be quantified together with brine. This result also supports the hypothesis that all SDS is distributed in microemulsion phase.

In the literature, Bellocq *et al.* [16] and Pouchelon *et al.* [17] studied the composition of the same systems over the entire range of Winsor. Gas chromatography and atomic absorption were used to quantify water, toluene and butanol and SDS in the systems at optimal salinity [16] or on Winsor I and Winsor II system [38]. By comparison, the quantification in the microemulsion phase of our Winsor I, Winsor III and Winsor II systems are in the same order that the ones reported as seen in *Table 3*. Nevertheless, in both studies n-butanol is found to be shared in the oil and aqueous excess phases in relatively small proportions (< ~4 vol.% in excess phase) depending on the studied salinity, oil/water ratio and amount of active species. With our method, no significant amount of n-butanol was detected in the excess phases, and so, for all samples. Indeed, the apparent and total densities profiles in the excess oil and aqueous phases were found to be equal to those of pure toluene and brine. This limit of detection is coherent and expected considering the precision of our method. To a greater extent, for real formulations that use ~ 1 to 2 % of active compounds or even model systems where cosurfactant is shared equally and in small amount between each phase [42,43], our method would potentially be limited to the quantification of oil and brine. In this case, actual quantification techniques would provide a more straightforward and precise access to mean volume fractions of surfactant and co-surfactant in the systems given a precision of 0.1%. Nevertheless, it is worth noting that mass balances were not reached in some of the quantifications of the given literature [16]. It could be explained by two reasons: i) the sampling procedure affects the quantification by transfer of species between the excess phases and the microemulsion and vice versa; ii) the use of different analytical techniques to quantify all compounds of a system.

In that sense, mass balances were performed to assess the accuracy of the determination of the volume fractions for each compound with NMR at the optimal salinity. In *Table 4*, volumes in mL were extracted from the average volumes fractions and phases thicknesses deduced from the densities profiles (Figure 7). The total volume was corrected by considering the meniscus effects at the oil/air and water/tube interfaces. We found a total volume of 3.06 mL compared to the 3.08 mL that were introduced initially. For each system, the remaining amount of n-butanol in the excess phases can be extracted (*Table 5*) by subtracting the volume fraction in middle phase from the introduced amount of n-butanol. The cosurfactant fraction in excess phases decreases from ~ 7 % to 0 % from Winsor I to Winsor II systems. Although this information is qualitative given the precision on n-butanol volume fraction (4 vol.%), we found the same trend in literature [17] where n-butanol in excess phases passes from 4.2 % to 1.6 % with increasing salinities. The increase of salinity leads to the concentration of n-butanol in the oil rich phase (microemulsion or excess oil phase).

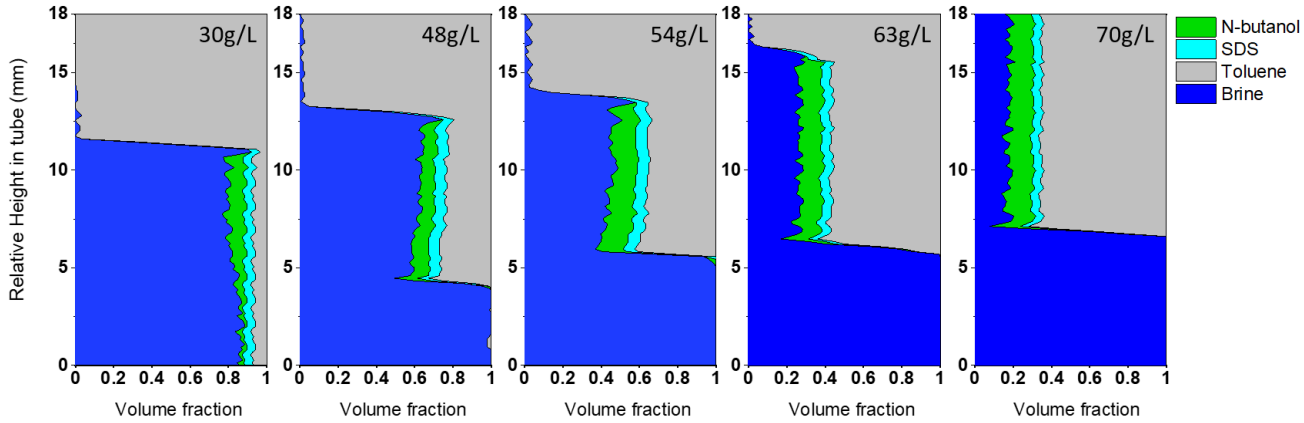

Figure 7 : Volume fractions in function of the relative height in tube for each species from NMR profiles at different salinities from Winsor I to Winsor III and Winsor II types of microemulsion. SDS was assessed under the hypothesis that all surfactants molecules are homogenously solubilized in the middle phase

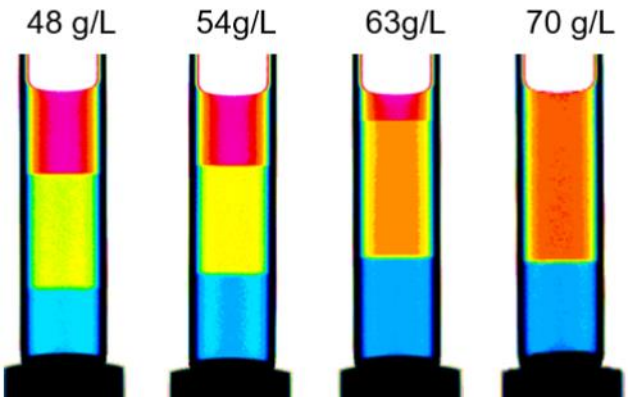

Figure 8 : Contrasted Micro-CT radiographies over the range of salinity – transition from Winsor I to Winsor II microemulsions

5 Conclusions

A method has been developed in Low-Field NMR to quantify locally the components in complex microemulsions systems without sampling. The work focuses on quaternary microemulsions made of NaCl brine/Toluene/n-butanol and Sodium Dodecylsulfate (SDS) over the full range of salinities (i.e. from Winsor I to Winsor III and Winsor II systems). The samples were studied at equilibrium in static conditions and compared to Micro-Computed Tomography data. We found that the method, with our input parameters, is not applicable to the detection of traces or small quantities lower than 4 vol.%. To allow data processing, we thus made the usual hypothesis that the SDS surfactant molecules are homogenously concentrated in the middle phase (i.e. bicontinuous phase). For the quantification of the three other compounds, we took advantage of contrasts in T_1-relaxation times as well as hydrogen densities between

n-butanol, toluene and brine. By studying the relaxation process in two modes: total and partial, the technique enables to quantify the local volume fractions of n-butanol, brine and toluene in the whole system. For Winsor III systems, the compositions were extracted with the minimum of deviations compared to Micro-CT (between 1 vol.% to 4 vol.%). Winsor I and II quantification led to an increase of the deviation on compositions compared to Micro-CT at optimal salinity (1 vol.% to ~ 7 vol.%). This precision would be sufficient if one needs to assess the overall partition of species in a complex system and/or even to follow their evolution over time. Overall, in the microemulsion phase (WI WII, WIII), good agreements are found over the entire range of salinities compared to the Micro-CT experiments and to the available literature. However, in the excess phases, we were not able to detect the co-surfactant given our method precision. Nevertheless, qualitative information could be provided thanks to mass balances. To conclude, the method presents several advantages because it is non-destructive, relatively fast, reproducible and can be adapted to opaque/dark systems. It gives simultaneous access to oil, brine and co-surfactant compositions, and so, in all types of microemulsions because it is slightly affected by the internal structure. This means that the developed method could potentially be extended to different colloidal systems insofar as the relaxation times are not strongly impacted by the structure of matter. Depending on the need of the application, the accuracy could be slightly enhanced by increasing the number of scans and dummy scans. Compared to other methods, the major drawback is that it does not allow the quantification of traces or small concentrations (< 4 vol.%) of chemicals and it requires a contrast in T_1-relaxation times and/or hydrogen index between each component of the system. In that sense, for a fine quantification of microemulsions, chromatography and chemical titrations remain the most straightforward techniques given a precision at 0.1%, with the main drawback of sampling.

It is worth mentioning that the work described in this paper was focused on species that have a monodispersed distribution of relaxation times. This is particularly not the case for viscous and multi-components fluids, like real crude oils for instance. The method could potentially be applicable even for large distributions of relaxation times depending on their polydispersity. However, in the case it is not, a solution would be to work at several relaxation delay values (RD) in the domain of partial relaxation mode. The integration of RD parameter would theoretically provide as many equations as needed to solve the system. Further studies need to be carried out in this way to assess practical feasibility. Regarding microemulsions, kinetics monitoring will be performed in a future work to have a better understanding of the diffusion mechanisms occurring during their formation.

Acknowledgements

The authors wish to thank Dr Elisabeth Rosenberg and Dr Maxime Pélerin from IFPEN (1 et 4 avenue de Bois-Préau, 92852 Rueil-Malmaison Cedex – France) for their assistance and support in the X-ray studies.

6 References

[1] Balinov B., Urdahl O., Soderman O., Sjoblom J., Characterization of water-in-crude emulsions by the NMR self diffusion technique, Colloids and Surfaces A: Physicochemical and Engineering Aspects 82 (1994) 173–181.

[2] Peña A. A., Hirasaki G. J., Enhanced characterization of oilfield emulsions via NMR diffusion and transverse relaxation experiments, Advances in Colloid and Interface Science 105 (2003) 103–150.

[3] Barrabino A., Keleşoğlu S., Sørland G. H., Simon S., Sjöblom J., Phase inversion in emulsions studied by low field NMR, Colloids and Surfaces A: Physicochemical and Engineering Aspects 443 (2014) 368–376.

[4] Marques D. S., Sørland G., Less S., Vilagines R., The application of pulse field gradient (PFG) NMR methods to characterize the efficiency of separation of water-in-crude oil emulsions, Journal of colloid and interface science 512 (2018) 361–368.

[5] Fiorotti T. A., Sad C. M.S., Castro E. R.V., Barbosa L. L., Rheological study of W/O emulsion by low field NMR, Journal of Petroleum Science and Engineering 176 (2019) 421–427.

[6] Montes L. F., Oliveira E. C.S., Neto Á. C., Menezes S. M.C., Castro E. R.V., Barbosa L. L., Low-field NMR, Fuel 239 (2019) 413–420.

[7] Nordgård E. L., Sørland G., Sjöblom J., Behavior of asphaltene model compounds at w/o interfaces, Langmuir the ACS journal of surfaces and colloids 26 (2010) 2352–2360.

[8] K.P. Mittal K.L. (Ed.), Handbook of microemulsion science and technology, Marcel Dekker, New York, 1999.

[9] Danielsson I., Lindman B., The definition of microemulsion, Colloids and Surfaces 3 (1981) 391–392.

[10] Wennerstrom H., Soderman O., Olsson U., Lindman B., Macroemulsions versus microemulsions, Colloids and Surfaces A: Physicochemical and Engineering Aspects 123-124 (1997) 13–26.

[11] Schwuger M-J., Stickdorn K., Schomacker R., Microemulsions in Technical Processes, Chemical reviews 95 (1995) 849–864.

[12] Winsor P.A, Hydrotropy, solubilisation and related emulsification processes, Trans. Faraday Soc. 44 (1948) 376–398.

[13] Broens M., Unsal E., Emulsification kinetics during quasi-miscible flow in dead-end pores, Advances in Water Resources 113 (2018) 13–22.

[14] Unsal E., Broens M., Armstrong R. T., Pore Scale Dynamics of Microemulsion Formation, Langmuir the ACS journal of surfaces and colloids 32 (2016) 7096–7108.

[15] Unsal E., Rücker M., Berg S., Bartels W. B., Bonnin A., Imaging of compositional gradients during in situ emulsification using X-ray micro-tomography, Journal of colloid and interface science 550 (2019) 159–169.
[16] Bellocq A.M, Biais J., Clin B., Fourche G., Lalanne P., Lemanceau B., Three-Dimensional Phase Diagram of the Brine-Toluene- Butanol- Sodium dodecylsulfate System, Journal of colloid and interface science 74 (1980) 311–321.
[17] Pouchelon A., Chatenay D., Meunier J., Langevin D., Origin of low interfacial tensions in systems involving microemulsion phases, Journal of colloid and interface science 82 (1981) 418–422.
[18] Pouchelon A., Meunier J., Langevin D., Chatenay D., Cazabat A.M., Low interfacial tensions in three-phase systems obtained with oil-water srfactant mixtures, Chemical physics letters 76 (1980) 277-281.
[19] Fukumoto A., Dalmazzone C., Frot D., Barré L., Noïk C, Investigation on Physical Properties and Morphologies of Microemulsions formed with Sodium dodecylbenzenesulfonate, Isobutanol, Brine, and Decane, Using Several Experimental Techniques, Energy Fuels 30 (2016) 4690–4698.
[20] Marquez R., Antón R., Vejar F., Salager J-L., Forgiarini A.M, New Interfacial Rheology Characteristics Measured Using a Spinning Drop Rheometer at the Optimum Formulation. Part 2. Surfactant-Oil-Water Systems with a High Volume of Middle-Phase Microemulsion, J Surfactants Deterg 22 (2019) 177–188.
[21] Chen S.-H., Rajagopalan R., Micellar Solutions and Microemulsions: Structure, Dynamics, and Statistical Thermodynamics, Springer International Publishing, Cham, 1990.
[22] Huie L., Zhanghui W., Jiange J., Jiankun H., Chuanqin Ding, Shuang C., Partition of n-Butanol among phases and solubilization ability of Winsor type III Microemulsions, J.Surfactants and Detergents (2016), 2016 713–724.
[23] Huie L., Pingping Z., Zhanghui W., Shuang C., Chuanqin D., Solubilization Behavior of Organic Mixtures in Optimum Winsor Type III Microemulsion Systems of Sodium dodecylsulfate, J. Surfactants and Detergents (2018), 2018 497–507.
[24] Hayes D. G., Ye R., Dunlap R. N., Anunciado D. B., Sai Venkatesh Pingali, O'Neill H. M., Urban V. S., Bicontinuous microemulsions as a biomembrane mimetic system for melittin, Biomembranes 1860 (2018) 624–632.
[25] Fukumoto A., Dalmazzone C., Frot D., Barré L., Noïk C., Characterization of Complex Crude Oil Microemulsions-DSC Contribution, Oil & Gas Science and Technology - Rev. IFP Energies nouvelles 73 (2018) 1–10.
[26] Dalmazzone C., Clausse D., Microcalorimetry, in: Marcel Dekker (Ed.), Encyclopedic Handbook of Emulsion Technology: J. Sjöblom, New York, 2001, pp. 327–347.
[27] Garti N., Aserin A., Tiunova I., Fanun M., A DSC study of water behavior in water-in-oil microemulsions stabilized by sucrose esters and butanol, Colloids and Surfaces A: Physicochemical and Engineering Aspects 170 (2000) 1–18.

[28] Lindman B., Olsson U., Wennerstroem H., Stilbs P., Comment on the self-diffusion in L3 and other bicontinuous surfactant solutions, Langmuir the ACS journal of surfaces and colloids 9 (1993) 625–626.
[29] Guering P., Etude structurale des microémulsions par effet Kerr et R.M.N.: Structural study of microemulsions by Kerr effect and NMR.
[30] Lindman B., Olsson U., Structure of Microemulsions Studied by NMR (1996).
[31] Fengping J., Zhishan B., Xiaoyong Y., Extraction of Mn(II) from NaCl solution by NaCl/sodium oleate/ n -pentanol/ n -heptane microemulsion system, Separation Science and Technology 53 (2018) 1351–1360.
[32] Tongtong X., Hongxing W., Aini Z., Nuojun Y., Ning L., Simultaneous Separation and Quantification of Vitamins by Microemulsion Liquid Chromatography, Journal of chromatographic science 58 (2020) 591–599.
[33] Schwarze M., Pogrzeba T., Volovych I., Schomäcker R., Microemulsion systems for catalytic reactions and processes, Catal. Sci. Technol. 5 (2015) 24–33.
[34] Hayes D. G., Ye R., Dunlap R. N., Matthew M. J., Sai Venkatesh Pingali, O'Neill H. M., Urban V. S., Protein extraction into the bicontinuous microemulsion phase of a Water/SDS/pentanol/dodecane winsor-III system, Colloids and surfaces. B, Biointerfaces 160 (2017) 144–153.
[35] Lawrence J., Rees G. D., Microemulsion-based media as novel drug delibery systems, Advanced Drug Delivery Review 45 (2000) 89–121.
[36] Kreilgaard M., Influence of microemulsions on cutaneous drug delivery, Advanced Drug Delivery Review 54 Suppl. 1 (2002) S77-S98.
[37] Hayes D.G., Pingali S.V., O'Neill H.M., Urban V.S., Ye R, Observation of a structural gradient in Winsor-III microemulsion systems, Soft matter 14 (2018) 5270–5276.
[38] D. Do L., Singh V., Chen L., Kibbey T. C. G., Gollahalli Sub. R., Sabatini David A., Algae, Canola, or Palm Oils—Diesel Microemulsion Fuels: Phase Behaviors, Viscosity, and Combustion Properties, International Journal of Green Energy 8 (2011) 748–767.
[39] Kayali I., Karaein M., Qamhieh K., Wadaah S., Ahmad W., Olsson U., Phase Behavior of Bicontinuous and Water/Diesel Fuel Microemulsions Using Nonionic Surfactants Combined with Hydrophilic Alcohol Ethoxylates, Journal of Dispersion Science and Technology 36 (2015) 10–17.
[40] Dantas Neto A. A., Fernandes M. R., Barros Neto E. L., Castro Dantas T. N., Moura M. C. P. A., Alternative fuels composed by blends of nonionic surfactant with diesel and water engine performance and emissions, Brazilian Journal of Chemical Engineering 28 (2011) 521–531.
[41] Bellocq A.M, Biais J., Bothorel P., clin B., Fourche G., Lalanne P., Lemaire B, Lemanceau B., Roux D, Microemulsions, Advances in Colloid and Interface Science 20 (1984) 167–272.
[42] Yu F., Jiang H., Fan Z., Xu F., Su H., Li J., Formation and Flow Behaviors of in Situ Emulsions in Heavy Oil Reservoirs, Energy Fuels 33 (2019) 5961–5970.

[43] Alzahid Y. A., Mostaghimi P., Walsh S. D.C., Armstrong R. T., Flow regimes during surfactant flooding, Fuel 236 (2019) 851–860.

Table 1 *Hydrogen index and transverse T_2 relaxation times for Toluene/Water/SDS/n-butanol*

Species	Hydrogen index	Relaxation time T2 (s)
Toluene	0.700	2.70
Water/Brine	0.980	2.93
SDS (in solution at 46.8 g/L)	1.020	2.54
N-butanol	1.013	1.13

Table 2 *Mean compositions (vol.%) and phase thickness of the equilibrated SDS/n-butanol/NaCl brine/Toluene microemulsion for the five salinities – from NMR and Micro-CT*

System	Type	Method	Brine	SDS	n-Butanol	Oil	Vol % of microemulsion in total system
30 g/L	Winsor I	NMR	77	4	6	13	65
48 g/L	Winsor I/Winsor II	NMR	56	6	7	31	47
		Micro-CT	60		40		43.2
54 g/L	Winsor III	NMR	40	6	12	42	44
		Micro-CT	47		53		41.1
63 g/L	Winsor III/Winsor II	NMR	22	5	11	62	53
		Micro-CT	31		69		52.3
70 g/L	Winsor II	NMR	14	4	13	69	61
		Micro-CT	25		75		65.4

Table 3 Mean compositions (wt.%) of the equilibrated SDS/n-butanol/NaCl brine/Toluene microemulsion for the five salinities – Comparison with NMR and Literature

System	Type	Method	Brine	SDS	n-Butanol	Oil
30 g/L	Winsor I	NMR	79	4	5	12
		Bellocq *et al.* [16]	88			10
50 g/L		Pouchelon et al. [17]	79	3	4	14
48 g/L	Winsor III	NMR	60	6	6	28
		Bellocq *et al.* [16]	84			14
54 g/L	Winsor III	NMR	43	6	10	41
60 g/L		Bellocq *et al.* [16]	38	5	6	48
63 g/L	Winsor III	NMR	24	5	10	61
		Bellocq *et al.*[16]	21			74
70 g/L	Winsor II	NMR	17	5	12	66
		Bellocq *et al.*[16]	14			69

80 g/L		Pouchelon *et al.*[17]	13	3	6	78

Table 4 *Mass Balances : volumes of n-butanol, water and oil deduced from NMR calculations compared to added volumes for the sample at optimal salinity of 54 g/L*

Calculated volume (mL)	**Excess oil**	**Middle phase**	**Excess aqueous phase**	**Total Calculated/Introduced**
N-butanol	0.00	0.14	0.00	0.14 / 0.17
SDS	0.00	0.07	0.00	0.07 / 0.07*
NaCl Brine 54g/L	0.00	0.52	0.77	(1.29 +0.14**) / 1.42
Toluene	0.59	0.48	0.00	(1.07 +0.13**) / 1.42
TOTAL				3.06 / 3.08

*Determined under hypothesis
**Corrected volumes

Table 5 *Qualitative information on the remaining volume fractions of n-butanol in excess phases (both aqueous and oil phases for Winsor III systems) obtained after mass balances calculations*

System	**Vol % N-butanol**
30 g/L	7.6
48 g/L	4.7
54 g/L	1.7
63 g/L	1.4
70 g/L	0.0